University of Exeter coursework header sheet

ECMM102 Group Project (Meng) (A, TRM1+2 2017/8)

Extension
059529

1029797

640003810

Coursework: Individual contribution to the group achievement
Submission Deadline: Mon 14th May 2018 12:00
Personal tutor: Professor Meiling Zhu

Marker name:	Tabor
Word count:	11,982

First marker's comments	Indicative mark
Second marker's comments	Second mark
Moderator's comments	Agreed mark

I2 Report

Investigation and Development of a Mathematical Model to Describe the Settling Characteristics of Olive Stone Powder

Aaron Wye

2018

4th Year MEng Group Project

I certify that all material in this thesis that is not my own work has been identified and that no material has been included for which a degree has previously been conferred on me.

Signed

College of Engineering, Mathematics, and Physical Sciences

University of Exeter

I2 Report

ECMM102

Title: Investigation and Development of a Mathematical Model to Describe the Settling Characteristics of Olive Stone Powder

Word Count: 11,982

Number of Pages: 40

Date of Submission: May 9, 2018

Student Name: Aaron Wye

Programme: MEng Mechanical Engineering

Student Number: 640003810

Candidate Number: 059529

Supervisor: Professor Gavin Tabor

Abstract

This report is part of a group project with the main aim of creating a validated Computational Fluid Dynamics (CFD) model of a Swirl-Flo® primary settling tank using Olive Stone Powder as a substitute for primary wastewater. The main aim of this individual report was to create a mathematical model that describes the settling behaviour of the powder. A secondary aim was to compare the behaviour of the powder with that of wastewater to evaluate its usefulness as a substitute. These aims were to be met through the completion of a series of experiments. For one of these experiments, a method of image processing was trialled to track the interface between the clarified water and the settled powder. It was found that this method was unsuccessful. It had a limited range of concentrations it worked for, and there is the potential the results have largely overestimated the settling velocity of the powder.

3 models in total were simulated: one for secondary wastewater taken from literature; one half powder, half wastewater; and one curve-fitted from the experimental results. It was found that the 2 models that were produced for the powder both significantly overestimated the settling velocity, with Model 3 producing the closest results. As such a fourth, much slower, settling model was produced, the simulation of which is ongoing.

The behaviour of the powder was compared to that of secondary wastewater as a basic qualitative comparison due to there being limited data for primary wastewater. It was found that the behaviour of the powder was only similar to the secondary wastewater for the sediment deposition near the inlet. This was to be expected as it should behave more like primary wastewater than secondary.

Keywords: Olive Stone Powder, Settling Velocity, Wastewater

Table of Contents

1 Introduction and Background

The use and reuse of water is a key environmental and sustainability issue faced in modern society. The UK government published in 2015 that by 2025 66% of the world's inhabitants could live in water stressed conditions [1]. As such, the efficient treatment of wastewater is becoming an increasingly important issue.

Wastewater treatment is generally split into 5 stages, shown as the blue boxes in Figure 1. This project focuses on the primary stage of wastewater separation which occurs after large debris screening and before the biological treatment in the secondary stage. During this stage, the wastewater is passed through settling tanks where gravitational settling occurs, removing $50 - 70\%$ of the total suspended solids [2]. These tanks tend to be large rectangular or radial settling tanks, however, the use of Hydrodynamic Vortex Separators (HDVS) is becoming more common due to their ability to handle higher Hydraulic Loading Rates (the volume of wastewater processed per unit area of the settling tank per unit time). HDVS combine gravitational settling with the effects of a vortex to aid the settling process and use faster flows, so a HDVS of smaller settling area can process more wastewater per unit time than a rectangular/radial tank.

Due to the nature of wastewater there is a great interest in the development of validated Computational Fluid Dynamics (CFD) models for use as an alternative to experimenting with raw wastewater. There is also an interest in finding a substitute that behaves the same as raw wastewater that could be used to improve safety when experiments are unavoidable. One such substitute that has been suggested and is investigated in this project is Olive Stone Powder. This is a commonly wasted by-product of olive oil production.

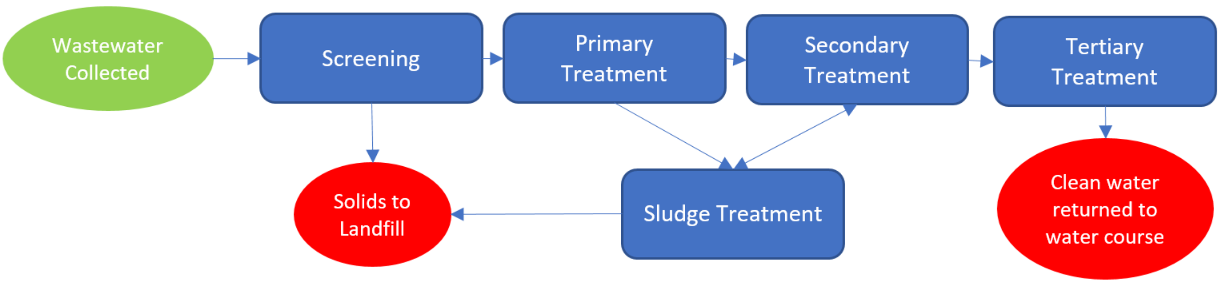

Figure 1: Image showing the stages in the wastewater treatment process. Recreated based on the stages in [3].

1.1 Group Project Aims

The group project was sponsored by Hydro International® with the main point of contact within the company being Dr Shenan Grossberg. The company provided a list of 9 key deliverables which are discussed in detail in the G2 report [4].

The main aim of the group project was to create a validated CFD model, using OpenFOAM®, for one of Hydro International®'s products, the Swirl-Flo® HDVS (referred henceforth as the 'Swirl-Flo®'). This would allow the company to produce optimised designs for the Swirl-Flo® without physical experiments which use large volumes of water.

There was also a secondary aim of evaluating whether Olive Stone Powder behaves as a substitute for wastewater. In order to do this it was required to determine suitable Settling Velocity and Rheology models to use within the CFD models.

1.2 Individual Project Aim

The aim of this individual section was to determine the settling velocity characteristics of the Olive Stone Powder suspended in the water. This led to the creation of 2 empirical equations relating the settling velocity to the concentration of powder. The resulting equations were to be used to support the group aim by enabling the settling of the Olive Stone Powder to be modelled correctly in the CFD simulations.

This aim was achieved through meeting several objectives. The first was an in-depth study into the theory related to settling behaviour. This led to the selection of a common wastewater settling model for use as a base for the empirical equation. The second objective was to research, select, and complete a series of experiments which would provide the relevant settling parameters for the powder. These parameters were then developed into 2 empirical formulae for the powder for comparison with results from experiments using the powder in a rectangular and Swirl-Flo® tank. The final objective was to determine which of the empirical models for the powder best represented its physical behaviour in the simulations, and to compare this to a model for secondary wastewater to see if the behaviour was similar. This comparison with secondary wastewater was necessary as there is limited data for primary wastewater so this provided a qualitative comparison to determine if the powder behaves as a suitable substitute for primary wastewater.

1.3 Report Structure

This report is split into 8 sections for clarity. This section (Section 1) contains an introduction to wastewater modelling, a description of the group and individual aims, and this guide to the report structure.

Sections 2 and 3 contain the Literature Review and the Theoretical Background respectively. The Literature Review contains an in depth review of what has been done previously and what is being done currently in the field of wastewater settling modelling and Olive Stone Powder modelling. Following on from this, the Theoretical Background section expands on the relevant concepts identified in the literature review with a major focus on the settling model selected as the basis for this report.

The main body of the project work is contained in Sections 4 and 5, the Methodology and Results respectively. The Methodology details all of the experimental work that was completed, and the results of these experiments are detailed in the Results section.

Section 6 contains the Discussions and the Conclusions of the project. The Discussions subsection contains analysis of all of the results and what they mean in terms of the validation of the settling velocity model. The Conclusions subsection summarises the pertinent points from this report and concludes on the success of the project as a whole. Also included in this section is a subsection with suggestions for further work which can be done off of the back of this report.

The final two sections of this report (7 and 8) detail the Project Management and the additional Contributions to the Group Functioning respectively. All references can be found in Section 9.

2 Literature review

Wastewater modelling is an area of research that has been covered in depth a lot over time, and has a large amount of ongoing research. This is due to the clear benefits of computational modelling; such as less experiments using raw wastewater, and the ability to test out new separator designs without having to manufacture them. However, the majority of this research focuses on secondary wastewater and not on primary. This trend is most likely due to the simplicity of primary wastewater separation; primarily gravitational settling in large tanks. This however is not the case with more modern primary treatments. Devices such as the Swirl-Flo® combine gravitational settling with the effects of a vortex to settle out solids with greater efficiency. This process is more complex and lends itself to a more thorough understanding of the wastewater settling behaviour [5].

Another big research area related to wastewater is the finding of suitable substitute substances that can be used to replicate the behaviour of raw wastewater. This is done to prevent the need to run experiments using raw wastewater. Different sources of wastewater require different substitutes to be used, this report looks at the use of Olive Stone Powder which has been used previously to model storm water runoff [6, 7, 8] (further discussed in Section 2.2). The results of mathematical models for wastewater tend to be validated against both experimental data using the substance and against full scale tanks using raw wastewater [6, 7, 9]. This validation process allows the model to be used further without the need for experiments. The model in this report is only validated against laboratory scale experimental data using the Olive Stone Powder. This means the validation done for it as a wastewater substitute is only partial, such as the validation shown in [8].

2.1 *Wastewater Settling Modelling*

The two parameters commonly required for wastewater modelling are the Rheology and the Settling Characteristics [10, 11]. This report focuses on the Settling Characteristics of the wastewater with the view to create a settling model for Olive Stone Powder. There are a large number of settling models available, a review of the ones up to 2015 is available in [12], all with varying degrees of complexity dependent on application.

One thing generally agreed upon is that the settling behaviour of wastewater can be split into four characteristic zones: Discrete, Flocculent, Hindered, and Compression Settling [2, 9, 13]. These zones are commonly accepted and form the basis of the majority of settling models. It depends on the concentrations of particles present as to what zones the models focus on. For applications where only high concentrations are involved only the Hindered and Compression zones are modelled. These use models such as the Richardson-Zaki model [14] and the Vesilind model [15]. These kinds of models produce good results for high concentrations, but tend to overestimate the settling velocity at lower concentrations [9].

In order to include the lower concentration behaviour, the Discrete and Flocculant zones, more complex models can be used. Models such as the *HTC* model by Ramin et al [11] contain multiple equations which are dependent on what concentration of wastewater is being used. This particular model was found to estimate the sludge bed accurately within a secondary settling tank, but overestimated the velocities for high concentrations. Another commonly used settling model is the *Double Exponential* model by Takacs et al [9] (which will be referred to as the 'Takacs model' for the rest of the report). This model has been used by multiple researchers to model the behaviour of wastewater [10, 13, 16]. The Takacs model uses a single equation to describe the behaviour of all four zones. It has been shown in [11] that the Takacs model produces similar, but slightly worse results, to the *HTC* model. It was decided for this project to use the Takacs model as a base for the Olive Stone Powder model. This was done so as to start simple and see whether the added complexity would be necessary if the simpler model did not work.

2.2 Olive Stone Powder Modelling

Olive Stone Powder is made by grinding olive stones that are a byproduct from the manufacturing of olive oil. The powder itself is most commonly used as an exfoliant in the cosmetic industry and can also be found in products such as paints and non-slip coatings. The powder is cheap and 100% bio-degradable. As such it is a desirable material to utilise. A common area of research is in the use of the powder as a low cost absorbent for wastewater treatment [17]; it is commonly used for heavy metals such as Nickel [18, 19].

This report focuses on the use of the powder as a substitute for wastewater. One of the earliest mentions of this is in a 1991 PhD by Ellis on optimising the self-cleansing operation of storm water storage tanks [6]. Storm water storage tanks are large tanks that are used to regulate excess flow in sewers. Within these tanks sedimentation occurs which was focused on in the study to prevent sediment build up. In Ellis' study, Olive Stone Powder was used as a substitute for the sewage wastewater in several laboratory scaled experiments, the results of which were used to compare with full-scale tank results.

An important conclusion from [6] is that the position and depth of the sediment of the powder in the laboratory experiments was similar to that of the full-scale tank, meaning the powder behaved as a suitable substitute in this case. However, it should be noted that Ellis stated that "*no exact flow record of the full scale chamber was available*". This means that assumptions were made for the flow behaviour in the full-scale tank and as such there is a potential for discrepancies based on any incorrect assumptions made. Ellis' study used an inlet concentration of powder that is similar to that of the experiments in this report, but the particle sizes are different. As such, the actual results from the work of Ellis are not directly comparable to those presented in this report. However, this initial use of the powder as a wastewater substitute can be used as a base for further validation of its use.

Another paper that uses Olive Stone Powder as a wastewater substitute in storm water storage tanks was produced by Stovin and Saul in 1994 [8], which is based on the use of the powder by Ellis. The purpose of this article was to produce an in-depth study into the sedimentation behaviour in the tank for different inlet conditions, focusing on the bed shear stress to determine the deposition of the powder. Stovin and Saul used the same grade of powder as is used in this report. However, the results of the laboratory experiments were not validated against any full-scale wastewater results so a valid conclusion on whether the powder behaves as a suitable wastewater substitute could not be determined.

Further to the work of Ellis, and of Stovin and Saul, a paper by Shepherd et. al. in 2008

[7] uses Olive Stone Powder in a rectangular settling tank to measure its retention efficiency. This is similar to the work done to meet the group aims in this project. The results of Shepherd et al's experiments with the powder were compared with classical sedimentation theory and a full-scale wastewater tank in the North-East of England. Shepherd et al concluded that the results from the experiments with Olive Stone Powder matched well to the results expected from classical sedimentation theory, and compared well with the full-scale tests.

Shepherd et al set a precedent for using Olive Stone Powder in laboratory experiments of settling tanks as a wastewater substitute. Its use as a wastewater substitute is further supported by the work of Ellis, and Stovin and Saul, however, there is a gap in the literature for further validation of its use in settling tanks. A particular gap in the literature for validation is its use in HDVS such as the Swirl-Flo® tank analysed in this report.

2.3 Conclusions From the Literature

By reviewing the literature, several important conclusions can be made. The most pertinent being that there is a gap in the literature for the project to investigate the behaviour of Olive Stone Powder as a substitute for primary wastewater. In particular it has been identified that there is no specific in-depth data regarding the settling characteristics of the powder. Also identified is the need to further validate whether the Olive Stone Powder is a good substitute for wastewater. To conclude on the validity of using the powder as a wastewater substitute it has been realised that a comparison of its settling characteristics against a common wastewater model would be valuable.

This report attempts to fill these gaps in the literature by modelling the settling characteristics of Olive Stone Powder using the commonly used Takacs model as a basis. This was then used for simulations on a rectangular and Swirl-Flo® tank and compared to experimental results to validate the Olive Stone Powder model. This model was then compared to one for wastewater, taken from [9], to provide a partial evaluation as to whether the powder acts as a wastewater substitute.

3 Theoretical Background

This section describes the theoretical background of the Takacs model and how it fits within the CFD solver used for this project. Section 3.1 describes in detail the model and the specific zones of interest within it. Section 3.2 describes where the settling model fits within the Drift Flux equations used for the simulations of the settling tanks.

Throughout this report the definition *Volume Fraction*, also called alpha (α), is used. This is related to concentration through the relationship shown in equation 1, where ρ_p is the particle density and the concentration is in mgl^{-1}. α is used in place of concentration as it is dimensionless which allows direct comparisons between particulates with different properties (such as density).

$$\alpha = \frac{Concentration}{1,000\rho_p} \tag{1}$$

3.1 *The Takacs Settling Model*

Published in 1991 by Takacs et al, [9], the Takacs settling model develops on the Vesilind model, [15], and describes the settling of wastewater inclusive of all of the four zones of settling behaviour identified in Section 2.1. It is a single equation model that has been extensively used and shown to produce good results in most cases.

The original formulation of the Takacs model can be found in [9]. This report focuses on the equation used within the CFD programme OpenFOAM® which is shown in equation 2.

$$\mathbf{U_{pj}} = \frac{\rho_f}{\rho_m} v_{ts} (e^{-a(\alpha - residualAlpha)} - e^{-a_1(\alpha - residualAlpha)}) \tag{2}$$

In this equation, $\mathbf{U_{pj}}$ is the vertical settling velocity of the particle phase, ρ_f is the density of the fluid, ρ_m is the combined density of the particle and fluid phases, v_{ts} is the maximum settling velocity, a is the low concentration settling parameter, a_1 is the hindered settling parameter, and $residualAlpha$ is the volume fraction of non-settling particles. The equation is also subject to the constraint $0 \leq \mathbf{U_{pj}} \leq v'_0$ where v'_0 is the maximum practical settling velocity. These parameters are explained in greater depth in the following subsections.

The Takacs model equation can be shown as a graphical relationship between settling velocity and the volume fraction of the particulates in the wastewater, as in Figure 2. It can be seen that the curve can be easily split into 4 zones of interest. These zones do not directly correspond to the 4 zones of settling behaviour from Section 2.1, but are closely related. These relationships are discussed in the following subsections.

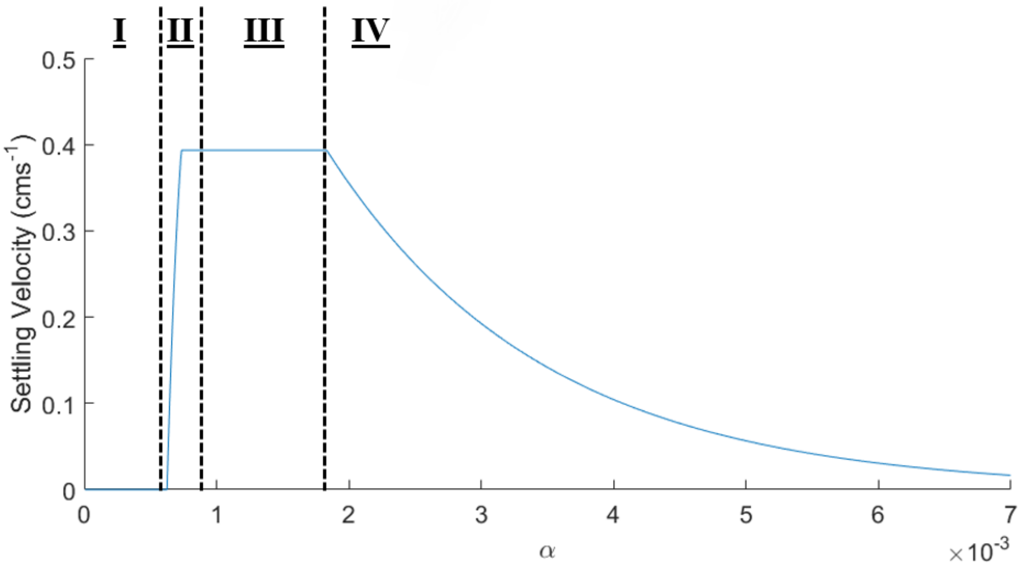

Figure 2: Graph showing the settling velocity relationship described by the Takacs settling velocity model. Recreated based on [9].

3.1.1 Zone I

Within Zone I of Figure 2 it can be seen that the settling velocity is zero. Within all suspensions, wastewater in particular, there are particles which either float or have very low settling velocities. These particles require removal from suspension in other ways which occur in processes after primary settling.

This region is characterised by the parameter $residualAlpha$ in equation 2, this is the α value for below which the settling velocity is zero and above which it is non-zero. The value for $residualAlpha$ is calculated using the concentration of the suspension entering the settling tank and can be found experimentally through the use of a Swing Column such as that used by

Tayak in [20]. The procedure for the Swing Column experiment is described in detail in Section 4.2.3.

3.1.2 Zone II

The behaviour of Zone II (seen in Figure 2) settling is explained primarily due to the effects of Flocculent settling. This is a behaviour that is observed for low α values with cohesive particles. As the volume fraction increases the likelihood of particles cohering together increases. This leads to larger *flocs* forming which increases the discrete settling velocity of the individual particles. This is due to the relationship between maximum discrete settling velocity and particle size, seen in the Stokes equation for discrete settling in equation 3. Here D_p is the diameter of the particle, μ_f is the dynamic viscosity of the fluid, and g is the gravitational constant.

$$v_{ts} = \frac{D_p^2(\rho_p - \rho_f)g}{18\mu_f} \tag{3}$$

This region is characterised in the Takacs model using the low concentration settling parameters, a. This parameter defines how steep the gradient of the curve in Zone II is. The determination of this value can be done experimentally by using Batch Settling experiments which are described in detail in Section 4.2.3.

3.1.3 Zone III

Within Zone III (seen in Figure 2) it can be seen that the settling velocity is invariant with α. This occurs due to the *flocs* reaching a maximum size and as such only discrete settling occurs. Discrete settling occurs when there are no inter-particle interactions, and as such the particles are free to settle at their maximum practical settling velocity, v_0'. It is important to note the difference between v_{ts} and v_0' at this point. v_{ts} is the maximum discrete settling velocity based on the size of the particles at the inlet, and v_0' is the maximum discrete settling velocity of the largest flocculated particle. Flocculation is difficult to predict due to the heavy reliance on flow patterns and cohesiveness. The way the Takacs model has characterised it through Zones

II and III has been referred to as a trick by Mazdeh in [21] that mimics the solution, and is not a fundamental solution. The value for v_0' can be determined empirically through Batch Settling experiments, detailed in Section 4.2.3.

3.1.4 Zone IV

The final zone in the Takacs model (Zone IV in Figure 2) describes the Hindered and Compression zones of settling identified in Section 2.1. At this point the model essentially reverts to the model created by Vesilind in [15]. Within this zone there is an exponential decrease in the settling velocity as α increases. This is due to the increase in inter-particle interactions; as the number of particles occupying a space increases the more they hinder the settling velocity of each other. As α gets large (i.e $\alpha > 0.008$ for this report) the settling velocity tends to zero. This area shows the compression settling which is often ignored in primary settling tanks as the high α sludge blanket is frequently removed.

This region is characterised by 2 parameters; the maximum discrete settling velocity, v_{ts}, and the hindered settling parameter, a_1. The value of v_{ts} is calculated theoretically based either on the Stokes settling velocity (equation 3) or the Newton settling velocity method (described in [22]) based on the value of the Particle Reynolds number, Re_p. The calculations done can be seen in section 5.1.1. The theoretical value can also be validated empirically using the Swing Column experiment described in Section 4.2.3. The value for a_1 is determined empirically through the use of the Batch Settling experiments described in Section 4.2.3.

3.2 The Drift Flux Equations

The Drift Flux equations are an alternative formulation of the Navier-Stokes equations that solves multi-phase flow problems by treating the 2 phases as a single mixture [23]. Within this mixture the properties of the different phases are defined related to their volume fraction, α. Any shared or combined properties are defined as *mixture quantities* and are created by combining the properties of the different phases together. The Drift Flux equations are derived from the Navier Stokes equations (full derivation available in [23]) based on these mixture quantities.

The three equations that are solved are shown in equations 4 to 6, taken from [13]. Equation 4 is the mixture continuity equations, equation 5 is the dispersed phase continuity equation, and equation 6 is the mixture momentum equation. In these equations U_m is the mixture velocity, τ is the shear stress, α_p is the particle volume fraction, M_m is the capillary force term, p_m is the mixture pressure term, and $\mathbf{U_{pj}}$ is the vertical settling velocity of the particle phase.

$$\frac{\partial \rho_m \mathbf{U}_m}{\partial t} + \nabla \cdot (\rho_m \mathbf{U}_m) = 0 \tag{4}$$

$$\frac{\partial \rho_m \mathbf{U}_m}{\partial t} + \nabla \cdot (\rho_m U_m U_m) = -\nabla p_m + \nabla \cdot (\tau + \tau^T) - \nabla \cdot (\frac{\alpha_p}{1-\alpha_p} \frac{\rho_f \rho_p}{\rho_m} U_{pj} U_{pj}) + \rho_m g + M_m \tag{5}$$

$$\frac{\partial \alpha_p}{\partial t} + \nabla \cdot (\alpha_p \mathbf{U}_m) = -\nabla \cdot (\frac{\alpha_p \rho_f}{\rho_m \mathbf{U}_{pj}}) + \nabla \cdot \Gamma \nabla \alpha_p \tag{6}$$

A fundamental assumption that is made in the Drift Flux model is that gravity is the main source of slip between the phases. This assumption means that the particle phase will travel both horizontally (driven by the flow) and vertically (driven by gravity). This makes this an ideal model for settling tanks where gravity is the primary driver of settling; with the addition of a vortex flow in the Swirl-Flo®.

The most important term to note from these equations for this report is $\mathbf{U_{pj}}$ which is in equations 5 and 6. This is the settling velocity of the particle phase in the vertical direction. This is the term that is modelled in this report. Within OpenFOAM® this term is defined by selecting the settling model as a *relativeVelocityModel* in the *transportProperties* dictionary. Within this it is possible to set the relevant parameters for the settling model. There are two default *relativeVelocityModels* within OpenFOAM®, one is the *simple* model which is a variation on the Vesilind model formulated by Dahl in [24] replacing the exponential with a base of 10. The model that is used for this project is the *general* model which is based on the Takacs model described in Section 3.1.

4 Experimental Methodology

This section of the report describes the overall methodology followed for the development and testing of the settling velocity models, starting with the determination of specific properties of the powder. First the powder properties were confirmed, then several parameters were found to define the settling properties of the powder. These settling parameters were then used to produce mathematical models for the settling of the Olive Stone Powder which were then tested.

4.1 Powder Properties

The supplier used for the Olive Stone Powder, *Goonvean Fibres*, provided the Product Data Sheet (PDS) [25] and the Material Safety Data Sheet (MSDS) [26] for the powder. These provided most of the information regarding the powder. However, two things required further investigation: the material density, and which particle grade to use.

The density for the Olive Stone Powder quoted on the MSDS was $440 - 770kgm^{-3}$ which was the bulk density. As such, it was necessary to carry out a simple experiment to find the material density of the particles. To do this a known mass of Olive Stone Powder was added to a known volume of water in a measuring cylinder and mixed. The mixture was left for 5 minutes and then the new volume in the cylinder was recorded. The density was calculated by dividing the change in mass by the volume displaced. The experiment was repeated 3 times and an average taken giving a value of material density for the Olive Stone Powder as $\mathbf{1438 \pm 103kgm^{-3}}$.

Goonvean Fibres provides 2 grades of Olive Stone Powder; *EFOG* or *OSF*. In order to determine which grade to use 2 methods were used; an experiment to see how they both behaved in water, and a comparison of the maximum theoretical settling velocity with literature values. The simple experiment was performed by mixing a set concentration of each of the powders and seeing how they behaved when settling. The *EFOG* particles settled out at a much higher rate than the *OSF* particles which led to the conclusion that the *OSF* particles behaved more like what would be expected for wastewater. This conclusion was further supported by the analysis of the maximum theoretical settling velocity which was found to be $0.0038ms^{-1}$ (calculated in

Section 5.1.1). This is within the range for wastewater given by Brennan in [10] of $0.0036 - 0.0083ms^{-1}$. Due to this it was decided to use the *OSF* grade powder.

4.2 Settling Parameter Determination

This section provides details of the methodologies used to find the required settling parameters for the Takacs model of the Olive Stone Powder.

4.2.1 Maximum Discrete Settling Velocity Calculations

The maximum discrete settling velocity, v_{ts}, is a value that can be calculated purely theoretically. To do this, either the Stokes equation, equation 3, or the Newton settling method, [22], is used depending on the value of the Particle Reynolds Number, Re_p. This is calculated using equation 7. If $Re_p < 1$ then the Stokes equation can be used, if not then Newton method should be used.

$$Re_p = \frac{\rho_f v_{ts} D_p}{\mu_f} \tag{7}$$

The assumption made for this report is that the powder particles are spherical. This was made on the basis of the observations made by Bennet et al in [28] that the shapes of the particles in ground Olive Stone Powder do not have large variations in aspect ratio. This was further supported by the work done in [27]. The decision to use only a single size of particle was also made due to the need to use a more computationally intensive Multiple Drift Flux Foam solver if there is a particle size distribution [29]. This meant there was no need to include shape functions or have multiple values for v_{ts}

4.2.2 Swing Column Experiment

In order to determine the value of the parameter $residualAlpha$ and to validate the theoretical value of v_{ts}, a Swing Column was used. The Swing Column used was supplied by Hydro International® in their labs in Clevedon. The setup is shown in Figure 3 with the two sample cells, A and B, labelled.

Figure 3: Image showing the Swing Column setup used at Hydro Internationals®' Labs.

The full procedure for the operation of the Swing Column was provided by Hydro International® in the form of a Work Instruction [30]. An outline of the most important steps is provided here.

To find the value for $residualAlpha$, first a value for the non settling percentage (f_{ns}) was found using the column. This was done by filling the column with a suspension of known concentration and leaving it for 3 hours locked into position with Cell B at the top. After this the column was turned and Cell B emptied. The powder in Cell B after this time is the powder that will not settle. From this, f_{ns} was found and then $residualAlpha$ could then be calculated using equation 8 where C_o is the inlet concentration in mgl^{-1}.

$$residualAlpha = \frac{C_0 f_{ns}}{1000\rho_p} \tag{8}$$

In order to validate the theoretical value for v_{ts} a settling velocity distribution was found from the Swing Column. To do this, after the 3 hours Cell B was refilled with clean water and the column positioned so Cell A was at the top. This was done as the powder that had settled in the 3 hours was concentrated in Cell A and hence would settle down to Cell B over the experiment time. Samples were taken from Cell B at specified time intervals and it was refilled with clean water after each sample. The settling velocity was determined by dividing the distance between Cells A and B by the time each sample was taken at. This then allowed a cumulative settling velocity distribution to be plotted.

All of the samples taken from the experiment were processed using the standard method for calculation of total suspended solids as outlined in [31]. The samples were filtered through pre-weighed filter papers, with the aid of vacuum flasks, and dried in an oven. The dried papers with the powder residue on were then weighed and the mass of powder found. This allowed the concentration of each sample to be found by dividing the mass change by the volume of the sample. This method was shown in laboratory testing on 77 known samples of $293mgl^{-1}$ to have a standard deviation of 7.235% [31].

The Swing Column test was carried out using 2 different concentrations, $300mgl^{-1}$ and $3000mgl^{-1}$. This was done to determine whether the initial concentration had an effect on the non settling percentage of the powder and the general distribution of settling velocities observed.

4.2.3 Batch Settling Experiments

One of the most commonly used settling experiments are the Batch Settling experiments, also known as zone settling experiments. This is because they can be used to characterise the settling behaviour of a suspension over the whole range of α. That being said, Batch Settling experiments are limited in range by the equipment that is available. From these experiments the values for a, a_1, and v_0' can be found.

Figure 4 shows the general expected clarification behaviour in a Batch Settling experiment. To find the settling behaviour the height of the interface labelled *Vs* in Figure 4 is measured at set time intervals and plotted against time. The first part of the graph should have a linear trend, the gradient of which is taken as the settling velocity for that concentration. Repeating this for multiple concentrations allows for the full graph of settling velocity against alpha to be plotted for the solution. From this graph it should be possible to curve fit in order to find the values for a, a_1, and v_0'.

To complete these experiments the Armfield W2 Sedimentation Studies apparatus were chosen and modified with extra light sources to improve the tracking of the interface (the final setup is shown in Figure 5). Through research it was found that the best way to track the interface would be through the use of a turbidity meter mounted in the base of the tube like the ones used by Ramin et al in [11]. However, due to budget constraints an alternative method was developed.

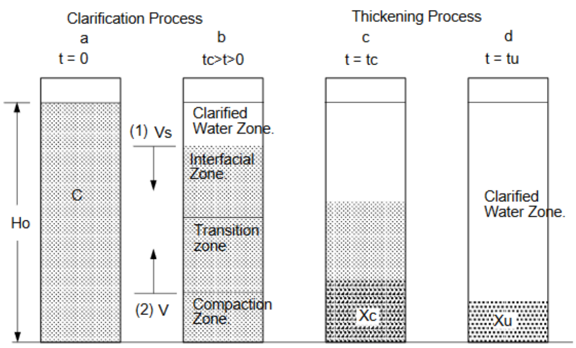

Figure 4: Image showing the clarification behaviour expected to be seen in a batch settling experiment, taken from [10].

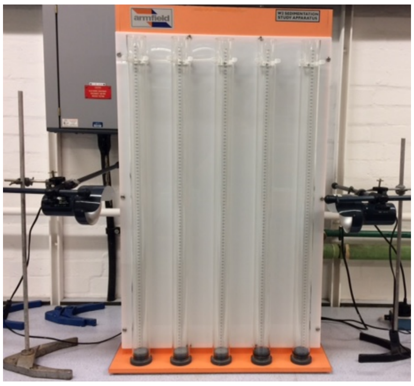

Figure 5: Image showing the Settling Tube setup used for the Batch Settling Experiments.

The alternative method developed for this report uses a digital camera to take images at set time intervals. These images were then processed through a MATLAB® script which initially converted the images to greyscale and then into binary images using the command *imbinarize*. This by default uses the Otsu method, [32], to automatically select a threshold value for where black and white are defined on the greyscale. An example of the binary image next to the original colour image can be seen in Figure 6. Two key things that needed to be kept constant in order to ensure that this method could be used was to make sure the images were taken from the same position each time and the external lighting was kept constant.

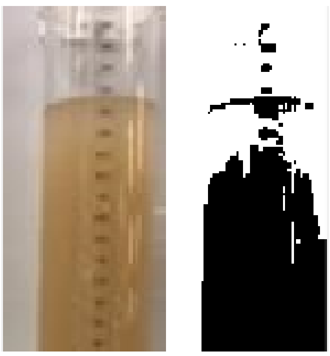

Figure 6: Image showing a close up of the interface region from the preliminary experiment at 30s. Shown is the binary image next to the coloured image to demonstrate the interface that has been found.

4.3 Model Development

A total of 3 models were used for this report. One was taken from literature as a secondary wastewater for comparison (no primary wastewater models were available), and 2 for the Olive Stone Powder. The details of the three models are listed here:

Model 1: Takacs Secondary Sludge Model, parameters taken from [9]
Model 2: Olive Stone Powder model using v_{ts} and $alphaResidual$ from experiments and a and a_1 from Secondary wastewater [9]
Model 3: Olive Stone Powder model curve fitted from the Batch Settling Experiments

Model 1 was used as a basis for a partial comparison between the powder and wastewater, to evaluate its usefulness as a substitute. Model 2 retains the wastewater values for a and a_1 as these two slopes would be expected to be similar to those of wastewater if the powder is a good substitute. Finally, Model 3 is produced entirely from a curve fit of the Batch Settling results, using the value for $alphaResidual$ found from the Swing Column. v_{ts} was changed for this model in order to allow the fit to work better. Model 3 was fit primarily within the range of interest, $\alpha < 0.007$, as this was the range of α values that was observed in preliminary simulations on the rectangular tank.

4.4 Model Testing

To test the mathematical models produced, 3 situations were simulated by the simulation team using OpenFOAM®. The first situation was a model of the settling tubes used in Section 4.2.3. Multiple concentrations were run to compare with the experimental results. From these simulations the interface can be tracked and compared with the batch settling experiment results to determine whether the fit for Model 3 behaves as expected.

The next 2 situations were the rectangular sedimentation tank and Swirl-Flo® tank simulations respectively. These simulations were more computationally expensive than the settling tubes. From these simulations the mass flow rate of the powder at the under and overflows as well as the sediment deposition were compared with experimental results. This was to determine which model most accurately modelled the powder. For the rectangular tank all 3 models were run, and for the Swirl-Flo® Model 2 was partially run due to computational limitations.

5 Results

This section displays the results of all of the experiments that were carried out to determine and test the settling velocity model. It is split into 3 sections: the first is the determining of the settling parameters; the second is the development of the model; and the final sub section is the results of the model testing and validation.

5.1 Settling Parameters

This section displays the results from the theoretical and experimental investigations that were followed in order to determine the settling parameters for the Olive Stone Powder that were required to fit the settling velocity model.

5.1.1 Maximum Discrete Settling Velocity

For the maximum particle size of $125\mu m$, found by Mendoza in [27], an initial estimate of the settling velocity was made using the Stokes equation (equation 3) and the corresponding value for Re_p was found using equation 7. This gave a value for v_{ts} of $0.0038ms^{-1}$ with a value of Re_p of 0.581 which meant that the Stokes equation holds. As such, the value for v_{ts} for the powder is $\mathbf{0.0038ms^{-1}}$.

5.1.2 Swing Column Experiment

As was described in Section 4.2.3, a Swing Column was used to determine the value of $alphaResidual$ and to validate the value found for v_{ts}. The results from the 3 hour test to find $alphaResidual$ are shown in Table 1. The results for both concentrations are shown including the calculation of the non settling percentage, f_{ns}. It can be seen that there was little variance between the two concentrations which implies the initial concentration does not greatly influence the value for f_{ns}.

Taking an average of the values for f_{ns} gives a value of $f_{ns} = 6.17 \pm 0.04\%$. This value was then converted into a value for $alphaResidual$ using equation 8. This gave a final value of $residualAlpha = \mathbf{1.28 \times 10^{-5} \pm 1.7 \times 10^{-6}}$ when using an inlet concentration of $300mgl^{-1}$.

Table 1: Table Showing the results for the non settling percentage from the Swing Column tests.

Concentration (mgl^{-1})	**Mass of Powder in Column (g)**	**Mass of Powder Floating after 3 hours (g)**	f_{ns} **(%)**
300	1.358 ± 0.0005	0.094 ± 0.0005	6.92 ± 0.04
3,000	12.763 ± 0.0005	0.690 ± 0.0005	5.41 ± 0.04

In order to validate the value for v_{ts} calculated theoretically in Section 5.1.1, Figure 7 was produced. This shows a cumulative distribution of the settling velocities observed during the 2 experiments. It can be seen that roughly 98% of the settled mass had a settling velocity less than the calculated value of v_{ts} of $0.38cms^{-1}$ for both of the concentrations tested. The 2% observed with greater settling velocities is potentially due to the small percentage of the powder that has a particle size of greater than $125\mu m$ or due to experimental error. The error bars in Figure 7 have been omitted due to them being too small to see in the plot.

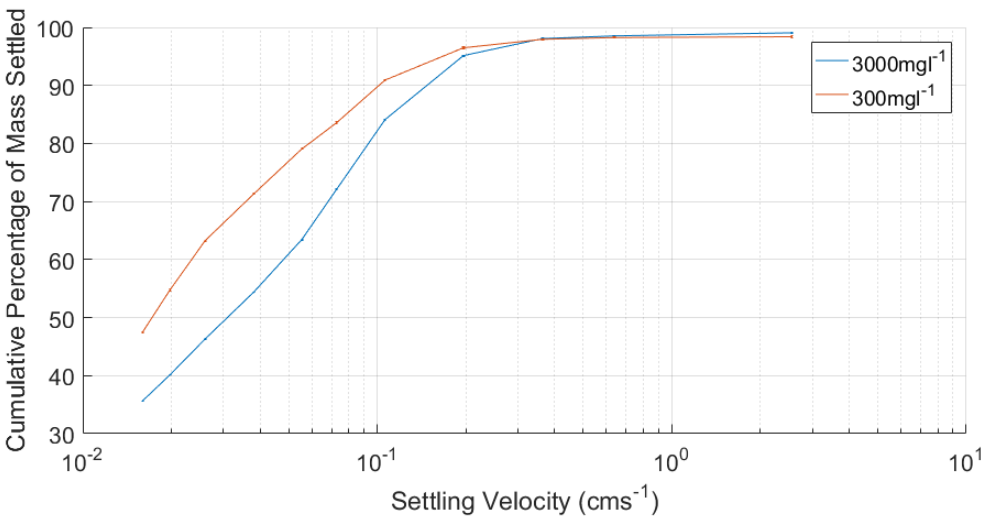

Figure 7: Graph showing the cumulative distribution of settling velocities observed during the Swing Column test.

5.1.3 Batch Settling Experiments

Using the methods outlined in Section 4.2.3, the Batch Settling experiments were run using 12 concentrations. Doing this identified a major limitation in the photographic interface tracking method used. It was not possible to pick up the interface for the 3 concentrations that were less than $540mgl^{-1}$. This presented an issue for the model produced from these results as the inlet concentration was $300mgl^{-1}$ which falls within the range of results that could not be found.

Figure 8 shows the raw interface results for 3 of the 9 concentrations that were run successfully. It can be seen that they follow the expected behaviour, with the linear region at the beginning. It was identified that the linear region occurred within the first 10 minutes for all of the processed concentrations.

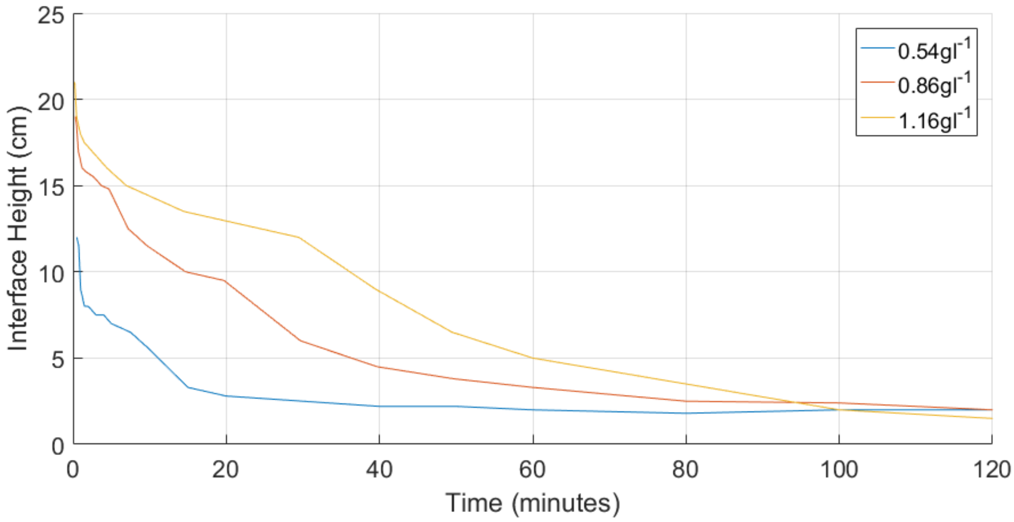

Figure 8: Graph showing the interface tracking results for 3 of the concentrations in the Batch Settling experiments.

From the raw data, the linear region was identified through maximising the value of the coefficient of determination, R^2, for the linear fit. The minimum value for R^2 for the linear fits was found to be 0.82 which is still a very strong linear fit. The gradients of these fits were found to give the settling velocity which was then plotted against α (concentrations were converted to α using equation 1). The results from this are displayed in Figure 9. The specific error in the tracking of the interface was difficult to quantify and as such is not included in the error bars and is considered a source of uncertainty in the overall reliability of the data. If the photographic method is validated further then this uncertainty could be nullified.

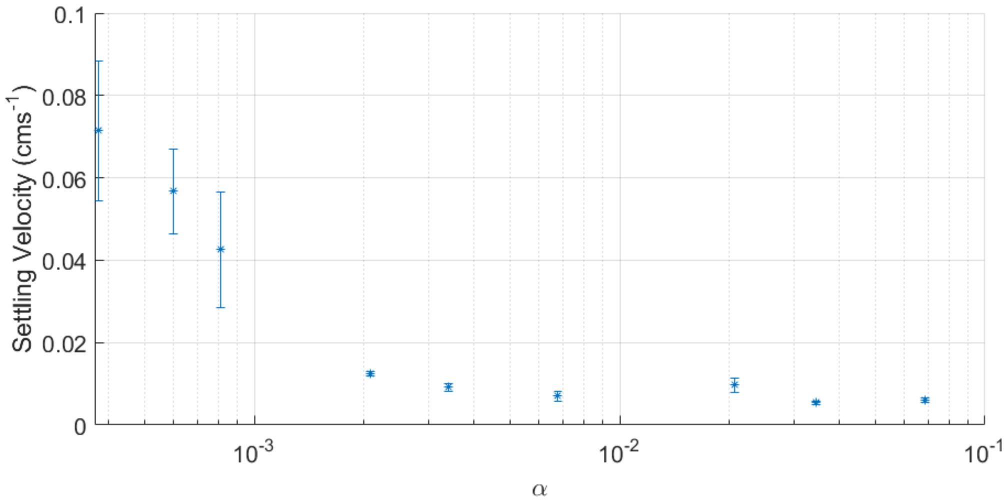

Figure 9: Graph showing the settling velocities found from the Batch Settling experiments.

It can be seen from the results that the general trend of the settling velocity behaviour shown is similar to what is expected, a decrease in settling velocity as α increases. However, the trend that can be seen is not solely exponential as was expected by the Takacs model for the hindered settling region. From these results it is possible to characterise the hindered settling behaviour of the Olive Stone Powder. However, it was not possible to characterise either the low concentration settling parameter, a, or the maximum practical settling velocity, v_0'. As such the results for a and v_0' are unknown and are estimated in the model fitting for the powder, discussed further in Section 5.2.1.

5.2 Model Development

A total of 3 models were fitted for this project, as listed in Section 4.3. The parameters that were found for each of the three models are presented in Table 2. These parameters were inputted into OpenFOAM® by changing the values within the *transportProperties* dictionary. The values for Model 1 were taken from literature for secondary sludge as there were no available primary sludge values, [9]. The values for a and a_1 for Model 2 were also taken from literature, [9], with the values for v_{ts} and $alphaResidual$ coming from the experiments and calculations carried out in the preceding sections. Models 2 and 3 do not contain values for v'_0 as it was not found experimentally and the value used in Model 1 was too high for both the Olive Stone models. A description of the curve fitting process to find the values for Model 3 is in Section 5.2.1.

Table 2: Table showing the parameters for the 3 settling velocity models that were found. These parameters were inputted into the *general RelativeVelocityModel* in OpenFOAM®

Parameter	Model 1	Model 2	Model 3
$alphaResidual$	2.09×10^{-8}	1.28×10^{-5}	1.28×10^{-5}
v_{ts} (ms^{-1})	0.00824	0.00380	0.00109
a	719.05	719.05	1064.12
a_1	7190.5	7190.5	10813.8
v'_0 (ms^{-1})	0.0039	–	–

The parameters defined in Table 2 correspond to the ones of the Takacs model in equation 2, and when inputted they can be plotted as shown in Figure 10. It can be seen clearly here the differences between the 3 models. Specifically how much lower the settling velocities are in Model 3 than in Model 2.

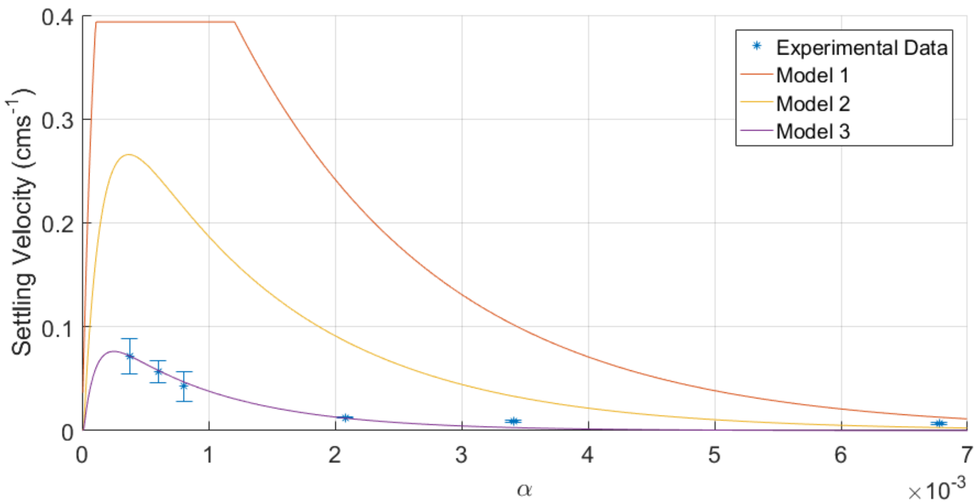

Figure 10: Graph showing the three settling velocity models plotted using the parameters listed in Table 2. These are plotted alongside the results from the Batch Settling experiments.

5.2.1 Curve Fitting Model 3

Initially, an attempt was made to fit an exponential trend to the results of the Batch Settling experiments using a MATLAB® fitting script. However, it was found that this was not possible over the whole data range. Specifically, for high values of alpha the results were found to fit to the power-law shown in equation 9 better than an exponential. Whereas, it was observed that the lower concentrations, $\alpha < 0.008$, fitted the exponential better.

$$v = 1 \times 10^{-5} \alpha^{-0.488} \tag{9}$$

As such, it was decided to fit the data only for the region of interest which was identified in Section 4.3, $\alpha < 0.007$. This decision was further validated by the fact it cut off the compression settling zone which is often not present in primary settling tanks. Doing this removed the power law region and allowed an exponential fitting of the hindered settling behaviour, characterised by a_1.

Due to the limitations in the Batch Settling experiments there was a large gap in the data between the experimental results and the region where the settling velocity is zero before $alphaResidual$. The missing region of results appeared to correspond to Zone II of the Takacs settling model. As such, an exponential increase was predicted and characterised by varying the value of a.

Only one parameter was fixed before the fitting process, this was the value for $alphaResidual$ found from the Swing Column results. The value of v_0' was not considered as it could not be determined experimentally. This left the values of v_{ts}, a, and a_1 that could be varied in order to fit the Takacs equation to the Batch Settling results. To find these parameters initial guesses were inputted by trial and error to move the fitted curve close to the experimental results. The initial value of v_{ts} was chosen to be $0.001ms^{-1}$ as this looked to be the area where the peak of the curve would be. After this values of $a = 1078$ and $a_1 = 11504$ were found to give a close fit.

After these initial guesses were found, optimisation tools within Microsoft Excel® were used in order to minimise both the average absolute error and the residual sum of squares. The absolute error was calculated by subtracting the model prediction from the experimental data, finding this as a percentage, and averaging this for all points. The residual sum of squares was found by squaring the absolute error of each point and summing these together. The average percentage absolute error gave a physical value for roughly how far off the model prediction was from reality, and the residual sum of squares was used to give a statistical value for how good the fit was. The use of the common R^2 value for quality of fit was suggested, but discounted due to its ineffectiveness on non-linear fits [33].

A combination of the *Goal Seek* and *Solver* functions of Microsoft Excel® were used to produce the final optimal parameters which can be seen in Table 2. These values gave an average percentage absolute error of 30.36% and a residual sum of squares value of $2.64 \times 10^{-8} m^2 s^{-2}$. The apparent high value of the average percentage absolute error is due to the two highest values of α in the region of interest which fitted closer to the power law plot than the exponential plot. However, the errors in the low α regions which are of more interest are very small. The residual sum of squares value is very small and hence indicates a close fit of the curve to the data points.

5.3 Model Testing

The following results are from experiments and simulations and are used to test and validate the models. They are also used to draw a conclusion of the usefulness of Olive Stone Powder as a wastewater substitute. All simulations were run by the simulation sub-group, meshes provided by the meshing sub-group, and the experimental results are from the experimental sub-group (which is the subgroup this report falls in). See [4] for sub-group member names.

5.3.1 Settling Tubes

Simulating the settling tubes showed that there was, as expected, a large dependence on what value of α was chosen as the interface as to how it behaved. Without knowing the exact value of α of the interface the experiments picked up, no meaningful conclusions could be found. It was however seen that the model in general behaved as would be expected for a settling tube.

5.3.2 Rectangular Tank

For this test, the results from the experiments ran on the rectangular tank were compared with the results of the equivalent simulations. The conditions for all results are $Q_{inlet} = 24.2lmin^{-1}$, $Q_{UnderFlow} = 1.3lmin^{-1}$, $Q_{OverFlow} = 22.9lmin^{-1}$, and $\alpha_{inlet} = 0.000208$ where Q is the flow rate. All measurements of sediment depth were done experimentally using a steel ruler with an error of $\pm 0.5mm$.

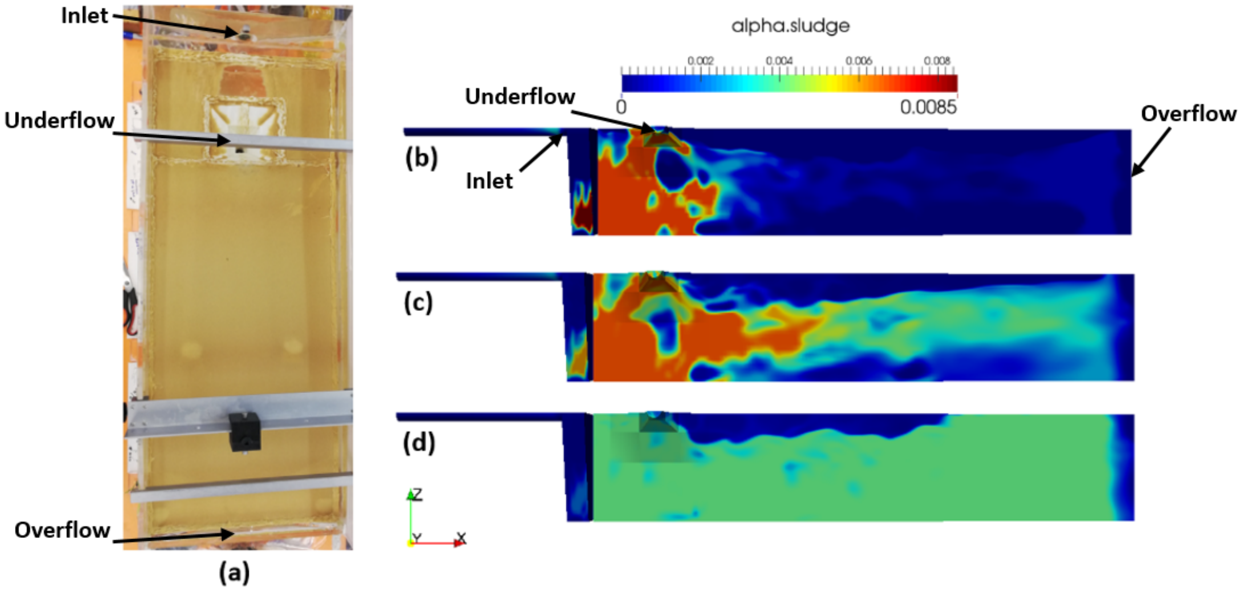

Figure 11: Images of the positions of the sediment in the rectangular tank. All 3 simulation results show the value of α for the sludge and use the same colour coding for direct comparison. The inlet, underflow and overflow are labelled on the images.
a) Top view of the experimental results taken after 2 hours 30 minutes.
b) Bottom view of the simulation using Model 1 taken at 10 minutes.
c) Bottom view of the simulation using Model 2 taken at 10 minutes.
d) Bottom view of the simulation using Model 3 taken at 10 minutes.

Figure 11 shows the areas where the sediment deposited in the inlet end of the tank from the experiment, and the simulations of the 3 settling models. The experimental results are displayed as a top view of the tank. The simulations are viewed from the bottom in order to see where the sediment has deposited. It can be seen that the majority of the sediment build up in the experiments is in the corner of the main tank at the inlet end ($1mm$ depth), this behaviour has been picked up by all 3 of the mathematical models. It can also be seen that the clearer section in the centre of the tank at the inlet end is also picked up by all 3 models, but with it being less noticeable in the Model 3 results. A direct comparison between sludge depths could not be made as the simulations were run over a 10 minute period and the experiments were run for roughly 3 hours each time. This meant the sludge heights measured in the experiments were taken after a long time build up. This was done because it was not possible to take sediment depth measurements in the middle of the experiments without disturbing the flow.

One obvious difference between the the results of the simulations and the experimental results is the difference in success of capturing the uniform bed on the sloped section. It can be seen that of the 3 models, Model 3 has picked this up best with Model 1 being the worst (as was expected as this is the model for secondary wastewater not the powder).

Presented in Table 3 are results for the overflow and underflow mass flow rates, the calculation of the experimental results and the associated errors is in [34]. It can be seen that for the Olive Stone Powder, Model 3 produces the best results. However, these results are still a factor of 10 out for both the over and under flows. This gives an initial indication that the model is overestimating the settling velocity of the powder. This is because the overflow is underestimated and the underflow is being overestimated indicating the powder is settling too fast.

Table 3: Table showing the results from the experiments and the 3 simulations for the rectangular tank.

Result	**Experimental**	**Model 1**	**Model 2**	**Model 3**
Overflow Mass Flow Rate (gs^{-1})	0.05 ± 0.0025	0.00125	0.003	0.0075
Underflow Mass Flow Rate (gs^{-1})	0.0055 ± 0.0007	0.03	0.028	0.025

Due to the large differences between the experimental and simulated results, a new model was developed. This model (Model 4) was developed to test the hypothesis that the settling velocity model needed to use slower velocities. This model is discussed in Section 6.2.

5.3.3 Swirl-Flo® Tank

Due to constraints in the computational time required to run simulations on the Swirl-Flo® tank no fully converged solutions were simulated. As such, no finalised simulation results can be presented here. The results of interest would have been the same as the ones presented for the rectangular tank for comparison. Figure 12 shows images from the experiments of the main regions of interest in terms of the sediment position and depth; the baffle plate, and the tray. The maximum depth on the baffle plate was found to be $7 - 10mm$ with a minimum depth of $1 - 2mm$ where there was measurable sediment. The maximum depth on the tray was found to be $0.5 - 1mm$ where there was sediment. From the experiments, the overflow mass flow rate was found to be $0.06 \pm 0.018gs^{-1}$ and the underflow mass flow rate was found to be $0.02 \pm 0.008gs^{-1}$. These values would be compared to the values from the simulations when available to determine if the mathematical model behaved as expected.

(a) (b)

Figure 12: Images taken from the experiments of the sediment deposition on the Swirl-Flo® tank:
a) The tray
b) The baffle plate

6 Discussions and Conclusion

This section is split into 4 sub-sections: general discussions on the results; details of the work that is ongoing; the conclusions that have been come to from this report; and a description of potential further work which could be of interest.

6.1 Discussions

All discussions in this section are based on the results gained from the experiments and simulations ran on the rectangular settling tank. This was done due to the computational time restraint meaning that the Swirl-Flo® simulations had not fully converged in time.

6.1.1 Olive Stone Powder Model Selection

When deciding which one of the Olive Stone Powder models (Models 2 and 3) behaved most like the physical experiments, there are 2 major things to consider. The first being where the sediment deposits, and the second being the mass flow rate of the powder at the over and under flows.

The sediment patterns for the experimental results, Model 2, and Model 3 can be seen in Figure 11, images a, c, and d respectively. There are 3 main characteristics that can be identified from the experimental results; the clear section in the centre of the tank by the inlet, the uniform sediment bed on the sloped section towards the overflow, and the build up of sediment in the corner of the tank at the inlet end. Model 2 shows the inlet end behaviour clearer than that of Model 3. This is potentially due to Model 3 having lower settling velocities and requiring longer for the pattern to show up clear enough on the scale used to compare between the models. However, on the overflow end of the tank, Model 3 produces more of the uniform pattern observed on the slope as in the experiments. It should also be noted that in the middle of the tank after the hopper there is a clear zone on both that is not seen in the experiments.

It can be said that in terms of the sediment patterns, neither of the models performed particularly well across the whole tank. However, there are slight differences between the experimental set-up and the simulation domain that could contribute to these discrepancies. In the experimental tank the new base had large lines of sealant along the joins, most prevalent around the hopper region. This sealant could be a cause of the uniform build up on the slope of the tank as the powder could not flow past the sealant down into the hopper properly. It could also be due to the particles settling too quickly in the simulations meaning they do not travel far enough up the tank in order to settle in the observed patterns in the experiments. This could be used as an argument for why either of the models produced better sediment patterns. As such it was decided to use the mass flow rates as the primary measure of comparison between the models.

The results for the mass flow rate for the experiments and Models 2 and 3 can be seen in Table 3. It can be seen that the results from both models are a factor of 10 out for both the experimental over and underflow mass flow rates. This is indicative of neither model behaving like the physical powder. Of the 2 results it can be seen that Model 3 predicts both the over and underflow mass flow rates marginally closer to the experiments than Model 2 does. It is observed that the models are both overestimating the underflow mass flow rate and underestimating the overflow mass flow rate. This observation is indicative of the particles settling too quickly in the simulations; most powder is going straight in and down into the underflow which is not what happened in the experiments. It can be seen that Model 3 predicts settling velocities lower than those of Model 2 (as can be seen in Figure 10) which is why it produces the better results for mass flow rate.

From the models presented thusfar for the powder (Models 2 and 3), it can be seen that the behaviour of Model 3 is slightly better than that of Model 2. Model 3 produces closer values for the mass flow rates out of the tank, produces most of the observed sediment pattern at the overflow end, but does not produce as clear sediment pattern at the inlet. However, neither model behaves particularly well and as such the work described in Section 6.2 is likely to produce a better model.

6.1.2 Evaluation of Photographic Interface Tracking Method

In terms of the use of the image processing trialled for tracking the interface for the Batch Settling experiments, it is found to be ineffective. The largest issue found with the method was the inability to capture the interface for concentrations lower than $540mgl^{-1}$. For this report that was a very large limitation as it did not allow for measurements to be taken in the region of interest, around the inlet concentration of $300mgl^{-1}$. This meant as there was no data in this region, large assumptions had to be made when curve fitting the results.

There is also the need to validate whether the interfaces picked up for the higher concentrations were correct. This comes from the observation made in Section 6.1.1 that Model 3 overestimated the settling velocities of the particles. If this is found to be true through the work described in Section 6.2 then it will be found that this method of interface tracking did not work. It is possible that if the settling velocities are found to be extremely low then the experiment could be run for longer and it might be found that the correct interface gets picked up later in the experiment. In order to potentially improve the results and potentially pick up the correct interface region, other threshold algorithms or better camera equipment could be used on longer experiments.

6.1.3 Olive Stone Powder - Wastewater Comparison

This section contains a basic, qualitative comparison between the behaviour of the Olive Stone Powder in the experiments against the simulation of the secondary wastewater model (Model 1). This comparison is made despite the projects focus on primary wastewater due to there being no available models, or equivalent experimental results available for the primary wastewater. This is a simple comparison based on the general behaviour observed.

Firstly, it can be seen that the mass flow rates of Model 1 are, much like Models 2 and 3, a factor of 10 away from the experimental values found. This implies that the secondary wastewater settles at a much greater rate than the Olive Stone Powder does. From the sediment patterns shown in Figure 11, it can be seen that the inlet end behaviour of Model 1 is very similar to that of the Olive Stone Powder experiments with the clear section in the middle and the build up in the corner. However, it can also be seen that the behaviour moving up the tank past the hopper does not resemble how the Olive Stone Powder behaved. This could potentially be due to the more rapid settling in the simulation not allowing enough particles to travel far enough up the tank to form the uniform layer seen in the experiments.

From this simple comparison it can be seen that the Olive Stone Powder does not behave like the secondary sludge beyond a similar sediment pattern in the inlet zone of the rectangular tank. However, this is to be expected as the powder is used to imitate primary sludge, not secondary. So, to form a more useful quantitative comparison of the powder with primary wastewater it would be necessary to compare the experimental results to a similar full-scale tank, or use a mathematical model for primary wastewater.

6.2 Ongoing Work

Due to the poor match between simulation and experimental results, discussed in Section 6.1.1, it was decided to test the theory that both Models 2 and 3 overestimated the settling velocity of the powder. To do this, a basic analysis of the parameters was carried out. It was decided that the relationship between a, a_1, or $residualAlpha$ and the mass flow rates would be too complex to analyse in the short time available for this. As such it was decided to focus only on the value for v_{ts}. It is obvious that the lower the value for v_{ts}, the lower the overall settling velocities are. From this it was decided to use an educated guess as to what a new value of v_{ts} should be. This was done to provide a proof of concept of the theory that the models needed to be slower. This is not meant to produce a high fidelity model that fits exactly to the powder.

It was seen that lowering the value of v_{ts} by 3.5 times from Model 2 to Model 3 led to an increase of the mass flow rate of 2.5 times. So using this logic it was decided to decrease the value of v_{ts} from Model 2 by 20 times to get the desired increase in overflow mass flow rate of 16 times. This led to the value of $v_{ts} = 0.00019ms^{-1}$. This value was used alongside the other parameter values for Model 3 (as it was the better model for the powder) and is currently being simulated on the rectangular tank geometry.

If the results from this proof of concept are accurate then it would be necessary to produce further studies into the remaining parameters to get the model to reproduce the physical behaviour of the powder. This work should be done alongside further empirical studies into the settling behaviour such as the ones described in Section 6.4. If the theory is incorrect then a further study of the settling behaviour would still be required with the potential for using a different settling model as a basis.

Currently, results for Model 4 for the first $50s$ of simulated time are looking positive. The underflow mass flow rate looks to be starting to converge within the correct order of magnitude and the overflow mass flow rate is continuing to increase, past the results seen from Models 2 and 3. However, the results are not fully converged so no final conclusions can be drawn.

6.3 Conclusion

From this report it can be concluded that the mathematical Model 3 for Olive Stone Powder produced more realistic results than Model 2 based on both the sediment pattern and the over and underflow mass flow rates. However, the results were still a factor of 10 out for both the over and underflow mass flow rates. The implication of this is that the models are overestimating the settling velocity of the powder. Testing of this theory is ongoing an summarised in Section 6.2.

It was also concluded that without improvement and validation, the photographic interface tracking method used for the Batch Settling experiments is ineffective. There is a limit to the concentration range, it would only work for concentrations greater than $540mgl^{-1}$. This was a fundamental flaw for this report as the concentration range of most interest was around $300mgl^{-1}$. This method would also be further invalidated if the outcomes of the ongoing work into the overestimation of the settling velocity is found to be true. This would imply the interface tracked in the images was not the correct one as it moved too quickly.

The final conclusion that could be made is based on the comparison that was made between the experimental results and the results of the secondary sludge settling model, Model 1. It can be seen that in terms of the sediment patterns observed, the powder appears to behave as would be expected of wastewater. However, the over and underflow mass flow rates for the powder were found to be a factor of 10 out for both from the simulated sludge model, this indicates that the powder settles slower than secondary sludge. This conclusion is based only on qualitative comparisons as the Olive Stone Powder is used as a primary sludge substitute so it would not be expected to behave as secondary sludge does.

6.4 Suggestions for Further Work

There is a large potential for further work to come from this report due to the ineffectiveness of the Olive Stone Powder models produced. The most obvious work would be to continue the proof of concept simulation described in Section 6.2. If the results show that the model does need to use lower settling velocities then it would be interesting to do an in-depth study into the effects the parameters other than v_{ts} have on the mass flow rate out of the tank and also the sediment patterns. If the results show that this is not the case then it would be worthwhile doing a further study using a different model from the Takacs model as a basis. From either outcome, it would be useful to do further empirical studies into the settling behaviour of the powder.

The experiments that would be of most interest would be the use of a settling tube, like the one used in this report, but with a turbidity meter mounted in the base like Ramin used in [11]. This would allow for a more accurate tracking of the interface height. Another experiment that would be of interest would be the use of Particle Image Velocimetry (PIV), such as in [35], to investigate the behaviour of the particles at low concentrations. This was the region which was not possible to measure for this report.

If it was decided that the photographic interface tracking method used in this report would be of use, there are several things that would be of interest to see if they can improve the results from it. The main one would be using a different method to define the threshold when converting the images from greyscale to binary. It would also be interesting the investigate the effect of the resolution of the images on the results. A final thing that could be tried would be the use of different dyes to soak the powder in to see whether different colours are picked up easier. Specifically, the use of a fluorescent dye could potentially be useful and the interface could be tracked based on the luminosity of the different regions.

7 Project Management

One of the most important aspects of project planning is time management. For this project planning was done on two levels; the higher level project plan managed at a group level, and the individual time planning. The individual time plan took the form of a Gantt chart with deadlines taken from the group plan in order to ensure key deliverables were delivered on time. To prevent individual setbacks affecting the group outcomes float time was included in the Gantt chart to anticipate any issues.

However, despite the included float time there were several setbacks to the project. One particular major setback which affected the whole group was the need to remodel the rectangular tank to make it fit for purpose. This required the manufacture of a new floor which nullified all previous work on the tank for the whole group. The effects of this setback were mitigated at a group level by pushing all individual activities back, utilising all remaining float time, to focus on the remodel. From a manufacturing perspective, this meant work was done on both tanks simultaneously in order to successfully catch up with the deadline.

Another setback that affected the groups progress was the servers that had OpenFOAM® installed went down several times during Term 2. This disruption stopped simulations running and did not allow access to any of OpenFOAM®'s utilities to visualise or process results. This led to the results from the simulations not being available until later than expected. The way of mitigating this was by writing reports without the results, in preparation for when the results could be processed and inputted.

Another important aspect that was considered was data management. Due to the Intellectual Property agreement with Hydro International® all documents regarding the project were stored on an online SharePoint provided by the company. All documents on the SharePoint were regularly backed up onto memory sticks in order to mitigate against any possible data losses. All experimental data that was taken was originally recorded within logbooks (to minimise use of computers near water) and was then uploaded to the SharePoint within a short period.

A final important aspect of the project planning was communication. Each week a formal meeting with the group supervisor, and an informal group update meeting were held. An agenda was produced for each of the formal meetings, in which a chair presided over the meeting with a secretary taking minutes. Additional notes from both the formal and informal meetings were taken in individual logbooks. Outside of meetings communication between the group members was done via online messenger services. Discussion with supervisors was done via email chains.

7.1 Health and Safety

There were several different parts of the project for which Health and Safety was a consideration. These centred mainly around the experiments performed within the fluids labs and the manufacturing completed within the student workshop. The work done within the fluids lab required a standard risk assessment for when using equipment near water, with the addition of the Olive Stone Powder and some use of solvent glues. As most of the manufacturing work completed in the student workshop was done with wood, the risk assessments required the use of a particle filter face mask (which was face fitted to prevent inhalation of sawdust) this was in addition to the normal Personal Protective Equipment used in the workshop. All of the relevant risk assessments were completed by the project safety officer and signed off by the project supervisor.

7.2 Sustainability Considerations

The overall group aim has sustainability at its centre. The creation of the validated CFD model could lead to a more efficient Swirl-Flo® device leading to an increase in the availability of clean water.

A sustainability concern that needed to be constantly addressed was the minimisation of how much dirty water was disposed of. In order to minimise this, tests of the equipment using dirty water was minimised. Tests such as leak tests were done using clean water. There was also an emphasis on not over-engineering any of the manufactured components, for each component the amount of material used was minimised.

8 Contribution to group functioning

This individual project fitted within the experimental sub-group of the project, [4]. The creation of a correct settling model for the powder was necessary to allow the simulations to accurately represent the experiments. This contributed to the global objectives of creating a validated simulation model for the Swirl-Flo® tank and concluding whether Olive Stone Powder is a suitable wastewater substitute.

In order to complete the objectives of this individual section, the work of both the experimental and simulation sub-groups was vital in testing whether the models produced work. By comparing the data from the experimental team with the simulation results for each of the three models produced it was possible to make conclusions on the accuracy of each model.

Additional to the development of the settling velocity model for the Olive Stone Powder, there were two further contributions to the group functioning. The first being the overall management of the project, and the second being the design and manufacture of items required to run the experiments on both the rectangular and the Swirl-Flo® tank.

8.1 Project Management

In order to ensure the smooth running of the overall project it was necessary to have a full overview of the progress of all of the key deliverables. This was primarily done through the making and monitoring of a project workflow diagram which was supported by a Gantt chart. The workflow diagram was produced as a flow-chart to give a visual interpretation of the interrelationship between the deliverables, it was monitored using different colours to define the progress on each section. The Gantt chart was used alongside this as a linear method of tracking the projects progress. Each of these were updated weekly after each group meeting. Further to this, it was necessary to keep track of the tasks assigned to each group member and ensure that they were able to complete what had been assigned to them to ensure a chain of responsibility.

Additional to this, the organisation of the groups SharePoint was also part of the project management responsibility. This involved creating and keeping organised different folders where all of the groups documents could be stored. All management documents are held on the SharePoint and are available to view on request.

8.2 Design and Manufacture

There were several key items that were required to design and manufacture in order to be able to run the experiments. These items were: the jigs for the measurement probes for both the rectangular and Swirl-Flo® tanks; the stands for the Swirl-Flo® tank and associated pipework; and the Rectangular tank floor and Hopper.

3 of these items were manufactured using the 3D printing facilities provided by the *FabLab* at the University of Exeter. These were the two Measurement Jigs and the Hopper for the rectangular tank floor. In order to make these, the components were designed and made in SOLIDWORKS® as solid parts and then exported as .STL files in order to be printed. These were then loaded into a stereo-lithography printers to be printed. The lead time on these parts was 2 days: one day for the print, and the other for the resin to cure and to remove support structures. The final printed parts are shown in Figure 13. The measurement jigs can be seen in images a) and b), and the printed hopper can be seen as the white component by the underflow in image c).

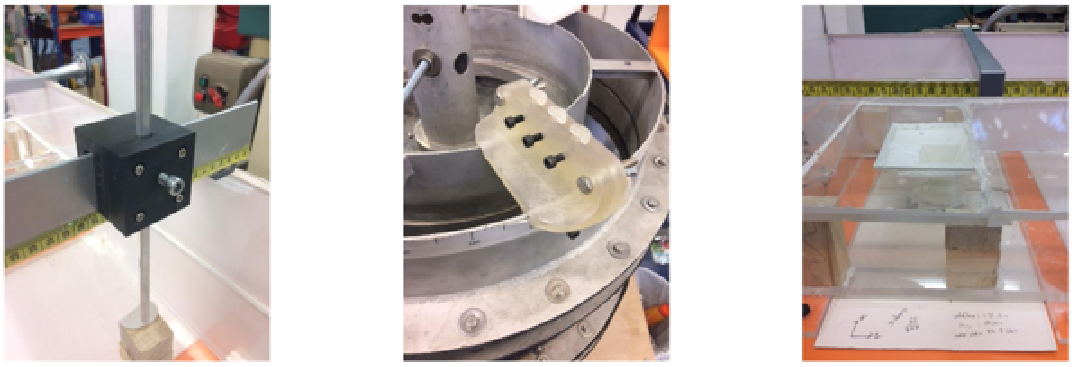
(a) (b) (c)

Figure 13: Images showing the components that were 3D printed for the project:
a) Rectangular Tank Measurement Jig
b) Swirl-Flo® Measurement Jig
c) Rectangular Tank Hopper

The other components that needed to be designed were the stands for the Swirl-Flo® tank and for the Pipes leading to it. These were designed using SOLIDWORKS® in order to get the correct measurements and to produce engineering drawings for the manufacture. The material chosen for the stands was wood as it is a versatile material that is easy to work with. The material choice was validated through a Finite Element (FE) simulation using ANSYS® workbench on the Swirl-Flo® stand. All material properties for both the CLS Pruce studwork timber used for the frame, and the marine-board plywood used for the top came from [36] and [37] respectively.

The results from the FE simulations were found after a mesh convergence was completed, this gave the optimum number of cells (around 100,0000 cells) required to give an accurate result whilst minimising computational cost. By doing this the maximum deformation on the stand was found to be 0.18mm and the maximum stress to be 6.2MPa. This was an allowable deformation size and the maximum stress was lower than the modulus of rupture of the wood (the stress at which the wood would fracture) of 45MPa. This gave a minimum factor of safety of 7 when considering the tank as weighing 217kg when filled with water. The stress result from the simulation can be seen in Figure 14, all other results including mesh convergence graphs are available on request. The stands were manufactured in the student wood workshop at the University of Exeter following all of the relevant health and safety guidelines. The final manufactured stands can be seen in Figure 15.

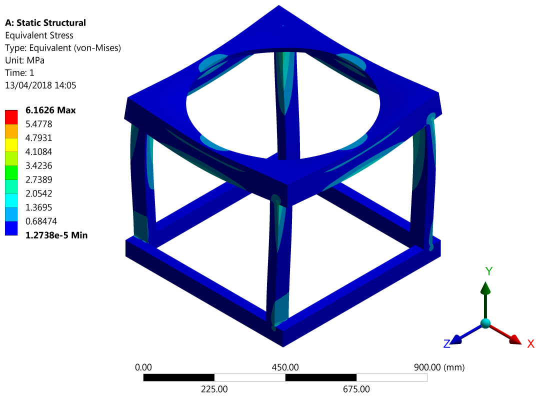

Figure 14: Image showing the stress results from the FE simulation. The maximum stress identified is 6.16MPa and is located on the base of the top where it meets the frames legs.

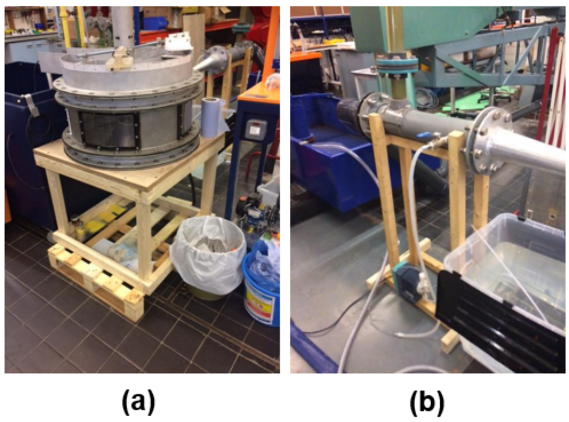

Figure 15: Images of the final manufactured stands:
a) Swirl-Flo® Stand.
b) Pipe Stand.

9 References

[1] Department for International Trade, *Water and Treated Water*, (11^{th} May 2015), https://www.gov.uk/government/publications/water-and-treated-water/water-and-treated-water, Last Accessed: [25/01/2018]

[2] Environmental Protection Agency, (1997), *Wastewater Treatment Manuals: Primary, Secondary, and Tertiary Treatment*, Environmental Protection Agency, Wexford, Ireland

[3] Water UK, *Wastewater*, (2018), https://www.water.org.uk/about-water-uk/wastewater, Last Accessed: [25/01/2018]

[4] A. Wye, A. Baker, J. Lowe, M. Mendoza, R. Bentley, T. Russell, and T. Scobell (2018), *G2 Report- Experimental and Numerical Investigation into the Use of Olive Stone Powder as a Substitute for Primary Sludge Modelling*, Group Dissertation (MEng), University of Exeter

[5] M. Faram, M. James, and C. Williams, (2004), *Wastewater Treatment Using Hydrodynamic Vortex Separators*, CIWEM 2nd National Conference, Wakefield, UK, Pages 79-87

[6] D. Ellis, (1991), *The Design of Storm Drainage Storage Tanks for Self-Cleansing Operation* Thesis (PhD), University of Manchester

[7] W. Shepherd, A. Saul, and J. Boxall, (2008), *Quantifying the Performance of Storm Tanks*, 11^{th} International Conference on Urban Drainage

[8] V. Stovin, and A. Saul, (1994), *Sedimentation in Storage Tank Structures*, Water Science and Technology, Volume 29, Issues 1-2, Pages 363-372

[9] I. Takacs, G. Patry, and D. Nolasco, (1991), *A Dynamic Model of the Clarification-Thickening Process*, Water Research Journal, Volume 25, Issue 10, pages 1263-1271

[10] D. Brennan, (2001), *The Numerical Simulation of Two-Phase Flows in Settling Tanks*, Thesis (PhD), Imperial College of Science, Technology , and Mechanical Engineering, London

[11] E. Ramin, D. Wagner, L. Yde, P. Binning, M. Rasmussen, P. Mikkelsen, and B. Plosz, (2014), *A new Settling Velocity Model to Describe Secondary Sedimentation*, Water Research Journal, Volume 66, Pages 447-458

[12] R. Silva, F. Garcia, P. Faia, and M. Rasteiro, (2015), *Settling Suspensions Flow Modelling: A Review*, KONA Powder and Particle Journal, Issue 32 , pages 41-56

[13] D. Ahern, (2017), *Study and Improvement of the Performance of an Industrial Settling Tank using CFD Models in OpenFOAM®*, Thesis (PhD), Universitat Politencia De Valencia

[14] R. Zaki, (1954), *Sedimentation and Fluidisation: Part 1*, Transactions of the Institute of Chemical Engineers, Issue 32, Pages 35-53

[15] P. Vesilind, (1968), *Theoretical Considerations: Design of Prototype Thickeners from Batch Settling Tests*, Water and Sewage Works Journal, Issue 115, Pages 302-307

[16] X. Liu, and M. Garcia, (2011), *Computational Fluid Dynamics Modelling for the Design of Large Primary Settling Tanks*, Journal of Hydraulic Engineering, Volume 137, Issue 3, Pages 343-355

[17] S. Pollard, G. Fowler, C, Sollars, and R. Perry, (1992), *Low-Cost Absorbents for Waste and Wastewater Treatment: a Review*, Science of the Total Environment, Volume 116, Issues 1-2, Pages 31-52

[18] T. Alsaibi, I. Abustan, M. Ahmad, and A. Foul, (2013), *Microwave Irradiated and Thermally Heated Olive Stone Activated for Nickel Absorption from Synthetic Wastewater: A Comparative Study*, AIChE Journal, Volume 60, Issue 1, Pages 237-250

[19] M. Martin-Lara, G. Blazquez, M. Trujilli, A. Perez, and M. Calero, (2014), *New Treatment of Real electroplating Wastewater containing Heavy Metal Ions by Absorption onto Olive Stone*, Journal of Cleaner Production, Volume 81, Pages 120-129

[20] J. Tayak, P. Hedges, and R. Smisson, (1996), *The Relationship Between Settling Velocity Grading and the Characteristics of the Contributing Catchment*, Water, Science, Technology, Volume 33, Issue 9, Pages 135-142

[21] F. Mazdeh, (2013-2014), *Investigating flocculation and discrete settling behaviour of activated sludge by means of particle size analysis*, Dissertation (MSc), Ghent University, Belgium

[22] NPTEL (National Programme on Technology Enhanced Learning), *Lecture 7, Settling and Sedimentation: Part 1*, http://nptel.ac.in/courses/103107084/module3/lecture7/lecture7.pdf, Last Accessed: [04/05/2018]

[23] M. Manninen, and V. Taivassalo, (1996), *On the Mixture Model for Multiphase Flow*, VTT Publications

[24] C. Dahl, (1995), *Numerical Modelling of Flow and Settling in Secondary Settling Tanks*, Thesis (PhD), Aalborg University Denmark

[25] Goonvean Fibres Ltd, (2016), *Product Data Sheet: OSF*, Issue 2

[26] Goonvean Fibres Ltd, (2016), *Safety Data Sheet: Ground Olive Stone*

[27] M. Mendoza, (2018), *Determination of a Viscosity Model for an Olive Stone Powder and Water Suspension for Primary Sedimentation Tank Modelling*, Individual Dissertation (MEng), University of Exeter

[28] J.C. Bennet, A.F. Koutsomitopoulou, A. Bergeret, and G.C Papanicolaou, (2014), *Preparation and characterisation of olive pit powder as a filler to PLA-matrix bio-composites*, Powder Technology, Issue 255, pages 10-16

[29] D. Burt, (2010), *Improved Design of Settling Tanks using an Improved Drift Flux Model*, PhD Thesis, University of Bristol

[30] Hydro International, (2014), *Work Instruction: Analysis of Settling Velocity Distributions*, Revision 1, WI PD No. 08

[31] American Public Health Association, (1995), *Standard Methods for the Examination of Water and Wastewater*, 19^{th} edition, Pages 218-224

[32] N. Otsu, (1979), *A Threshold Selection Method from Gray-Level Histograms*, IEEE Transactions on Systems, Man, and Cyberntetics, Volume 9, Issue 1, Pages 62-66

[33] A. Spiess, and N. Neumeyer, (2010), *An evaluation of R-squared as an inadequate measure of nonlinear models in pharmacological and biochemical research: a Monte Carlo approach*, BioMed Central Pharmacology, Open Access Article

[34] A. Baker, (2018), *Validation of Sedimentation Tanks through empirical Studies*, Individual Dissertation (MEng), University of Exeter

[35] L. Guo, D. Zhang, D. Xu, and Y. Chen, (2009), *An experimental study of low concentration sludge settling velocity under turbulent condition* Water Research Journal, Volume 43, Issue 9, Pages 2383-2390

[36] MatWeb, *Spruce Pine Wood*, (2018), http://www.matweb.com/search/DataSheet.aspx?MatGUID=3090e161c6384f119f69e2d93c369476&ckck=1, Last Accessed: [13/04/2018]

[37] MatWeb, *Douglas-Fir Plywood*, (2018), http://www.matweb.com/search/datasheet.aspx?MatGUID=6ce85c538d5843fd9dcbddc9dc22a011, Last Accessed: [13/04/2018]